

Demonstration of Near-Size-Independent External Quantum Efficiency for 368 nm UV Micro-LEDs

Guangying Wang,^{*} Shuwen Xie, Yuting Li, Wentao Zhang, Jonathan Vigen, Timothy Shih, Qinchen Lin, Jiarui Gong, Zhenqiang Ma, Shubhra S Pasayat, and Chirag Gupta

UV-ranged micro-LEDs are being explored for numerous applications due to their high stability and power efficiency. However, previous reports have shown reduced external quantum efficiency (EQE) and increased leakage current due to the increase in surface-to-volume ratio with a decrease in the micro-LED size. Herein, the size-related performance for UV-A micro-LEDs, ranging from 8×8 to $100 \times 100 \mu\text{m}^2$, is studied. These devices exhibit reduced leakage current with the implementation of atomic layer deposition-based sidewall passivation. A systematic EQE comparison is performed with minimal leakage current and a size-independent on-wafer EQE of around 5.5% is obtained. Smaller sized devices experimentally show enhanced EQE at high current density due to their improved heat dissipation capabilities. To the best of authors' knowledge, this is the highest reported on-wafer EQE demonstrated in $<10 \mu\text{m}$ dimensioned 368 nm UV LEDs.

1. Introduction

III-Nitride materials have been favored for UV range (200–400 nm) optoelectronics devices (LEDs and lasers) due to their advantages in efficiency, compact sizes, and being environmentally friendly compared to other UV emitters.^[1–4] With the increasing need for higher performance from UV emitters, micro-LEDs (chip size $<100 \mu\text{m}$) are becoming an important research direction due to their outstanding performance.^[5–7] Micro-LEDs have the potential to show higher stability under high current density while providing a higher light extraction efficiency and output power than regular-sized devices due to improved heat dissipation and reduced strain with decreasing device sizes.^[8–12] However, the surface area-to-volume ratio also

increases along with the decrease in the device size, which makes the sidewall damage become prevalent and results in poor electrical and optical properties as the device size is scaled down. This makes it difficult for micro-LEDs to outperform regular-sized LEDs.^[13] Currently, the theoretical efficiency advantages of smaller sized micro-LEDs have not been demonstrated experimentally; instead, often a lower external quantum efficiency (EQE) is observed for micro-LEDs compared to regular-sized LEDs,^[14] thus leaving room for further improvement of micro-LEDs' EQE.

On the other hand, micro-LEDs have been extensively studied for both visible wavelengths ($>420 \text{ nm}$), such as blue micro-LEDs,^[15–17] green micro-LEDs,^[18,19] and red micro-LEDs,^[20,21] and short wave-


length UV-C range ($<280 \text{ nm}$) micro-LEDs.^[22–24] However, very few studies have been done on the UV-A range (315–400 nm) with limited reports on the performance of micro-LEDs sized $<20 \mu\text{m}$. UV-A LEDs can be used in various applications such as curing, disinfection, lithography, counterfeit detection, and 3D printing.^[25] Recently, UV-A micro-LEDs are also being explored as a backlight source for color conversion-based display applications.^[26,27] With optimizations in the device designs and fabrication procedures, micro-LEDs can potentially achieve similar device efficiency as the regular-sized devices, which will make their advantage in heat dissipation and ability to hold higher power more prevalent. Therefore, UV-A micro-LEDs are quickly becoming extremely important for numerous applications.

UV-A micro-LEDs ($\approx 365 \text{ nm}$) with device sizes ranging from 3 to $60 \mu\text{m}$ have been studied for their electrical properties and junction temperature, demonstrating a thermal advantage. However, optical characteristics including EQE for micro-LEDs were not discussed in detail.^[10,11,14,28] Understanding both electrical and optical behaviors across different device sizes is critical for the advancement of device performance. This motivated us to perform a size-dependent study to examine the effect of device size on both the electrical and optical performance of UV-A micro-LEDs.

In this work, we have fabricated $8\text{--}100 \mu\text{m}$ sized square-shaped micro-LEDs on metal-organic chemical vapor deposition (MOCVD)-grown UV-A wafers with a stable emission wavelength of 368 nm. For the first time, we have demonstrated nearly size-independent EQE for UV-A micro-LEDs down to a size of

G. Wang, S. Xie, Y. Li, W. Zhang, T. Shih, Q. Lin, J. Gong, Z. Ma, S. S. Pasayat, C. Gupta
 Department of Electrical and Computer Engineering
 University of Wisconsin-Madison
 Madison, WI 53706, USA
 E-mail: gwang265@wisc.edu

J. Vigen
 Department of Material Science and Engineering
 University of Wisconsin-Madison
 Madison, WI 53706, USA

 The ORCID identification number(s) for the author(s) of this article can be found under <https://doi.org/10.1002/pssr.202400119>.

DOI: 10.1002/pssr.202400119

8 μm . Furthermore, to the best of authors' knowledge, we have demonstrated the highest on-wafer EQE ($>5\%$) for UV-A micro-LEDs with device size $<10\ \mu\text{m}$. Therefore, these results show the potential of UV micro-LEDs for display as well as other relevant applications.

2. Experimental Section

The epitaxial structure was deposited by MOCVD and is shown in **Figure 1**. The micro-LED fabrication process started with native oxide removal using a 1:1 (volume ratio) solution of hydrochloric acid and deionized water. Subsequently, 100 nm of Ni as *p*-type ohmic contact was deposited. Mesa pattern for n-contact was defined by a dry etch process after patterning with a photoresist. GaN dry etch was performed using a low-power Cl_2/Ar plasma chemistry.^[29] The devices were then passivated with 30 nm of Al_2O_3 using atomic layer deposition (ALD) and 270 nm of SiN_x using plasma-enhanced chemical vapor deposition. The deposition temperature of Al_2O_3 is 250 $^\circ\text{C}$ with trimethylaluminum as precursor. Via etching was performed on Al_2O_3 and SiN_x in the n- and *p*-contact regions. Finally, 50 nm/250 nm Ti/Ni was deposited by an electron beam evaporator as the n-contact.

In this work, current density (*J*)-voltage (*V*) measurements were performed by using Keithley 4200 semiconductor characterization system. On-wafer electroluminescence (EL) measurements were conducted on the backside of the sample through the sapphire substrate. The light was collected by a cosine corrector (Ocean Insight CC-3-UV-S) into the Horiba iHR320 spectrometer through an optical fiber. EL spectra were obtained through the combined use of the iHR320 spectrometer and a thermoelectrically cooled CCD detector (Horiba Synapse CCD) with a procedure involving a radiometric calibrated light source (Ocean Insight DH-3P-CAL). EQE versus *J* plot was obtained based on calibrated EL measurement system and Equation (1). EQE slope is utilized to quantify and predict the EQE droop across different device sizes. And the EQE slope from 100 A cm^{-2} (*J*₁) to 200 A cm^{-2} (*J*₂) is calculated by Equation (2).

$$\text{EQE}(\%) = \frac{\text{Emitted photon}}{\text{Injected electron}} \times 100\% \quad (1)$$

$$\text{EQE slope} = \frac{\text{EQE at } J_2 - \text{EQE at } J_1}{(J_2 - J_1)} \quad (2)$$

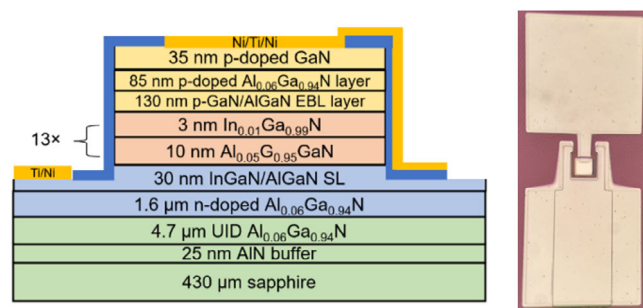


Figure 1. Cross-sectional schematic of UV-A LED with optical microscope image.

3. Results and Discussion

Micro-LEDs were fabricated into 8×8 , 15×15 , 60×60 , 80×80 , and $100 \times 100\ \mu\text{m}^2$ square-shaped devices. *J*-*V* measurement was performed on these micro-LEDs devices to evaluate the effect of the ALD sidewall passivation. Theoretically, with the decrease in the micro-LED size, the surface-to-volume ratio of the device will increase. This increase in surface-to-volume ratio can result in a higher leakage current in smaller sized micro-LED devices due to higher sidewall recombination.^[13] Sidewall passivation has proven to be effective in visible micro-LEDs improving sidewall defects and reducing current leakage. However, the extent of successful suppression of leakage current varies significantly between different studies.^[17,18,30] With sidewall passivation applied to 368 nm UV micro-LEDs, as shown in **Figure 2**, low reverse and forward leakage was observed in all micro-LEDs. Compared to 100 μm sized LEDs, approximately one to two orders of magnitude higher reverse leakage current were observed in 8 and 15 μm sized micro-LEDs. Nevertheless, the overall leakage current ($10^{-5}\ \text{A cm}^{-2}$) was still significantly low. The low forward leakage in all devices indicates suppression of carrier recombination caused by defects through an optimized passivation process.^[29–31] During forward bias after turn-on, devices with smaller sizes showed higher current density at all voltages (inset, Figure 2). This behavior might be due to the reduced current crowding and improved heat dissipation in smaller sized micro-LEDs. Similar phenomenon has been observed by other researchers as well.^[8,32,33]

In addition, EL spectra of all device sizes showed high uniformity with a peak emission with a length of $368.5 \pm 0.2\ \text{nm}$ and a full wave half maximum (FWHM) of $14.6 \pm 0.2\ \text{nm}$. 8×8 and $100 \times 100\ \mu\text{m}^2$ devices are shown in **Figure 3a,b**, respectively. Our measurement setup's intensity limitations make it challenging to uniformly measure all current densities with the same exposure time while keeping the intensities within reasonable limits. For instance, a current density of $10\ \text{A cm}^{-2}$ for a device size of $8 \times 8\ \mu\text{m}^2$ can be measured with a 10 s exposure time. However, at a current density of $50\ \text{A cm}^{-2}$, using a 10 s exposure time leads to spectrum saturation. Consequently, an adjusted exposure time of 2 s was necessary for accurate measurement. Because of these differences in exposure time, the intensity

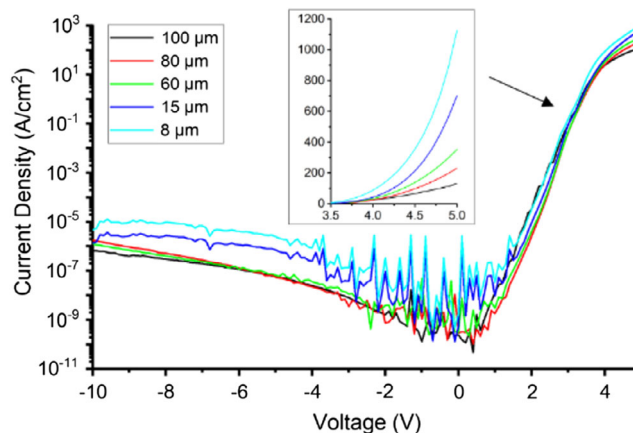


Figure 2. Current density versus voltage with voltage sweep of -10 to $5\ \text{V}$.

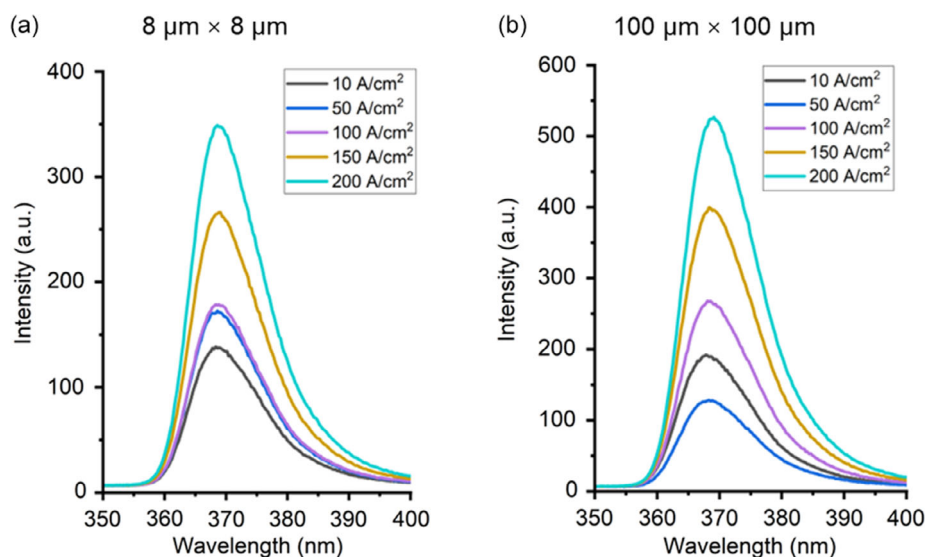


Figure 3. Electroluminescence spectrum with current density from 10 to 200 A cm⁻² of a) 8 × 8 μm² device with exposure time 10, 2, 1, 1, and 1 s, respectively, and b) 100 × 100 μm² device with exposure time 0.1, 0.01, 0.01, 0.01, and 0.01 s, respectively.

comparison may not be accurate among all different current densities. Peak emission wavelength and FWHM were influenced majorly through epitaxial growth conditions, and therefore independent of size. With increasing current density from 10 A cm⁻² to 200 A cm⁻², the peak emission wavelength shifted within 0.028 nm, which is very close to the detection limit.

These UV-A LEDs were designed with minimal indium concentration (<1.5%) in the quantum well. This low indium concentration results in less indium segregation which increases the composition uniformity of the wafer, hence leading to low FWHM and stable emission wavelength.^[34,35] Low indium concentration also decreases the quantum-confined Stark effect caused by InGaN/AlGaN interface,^[36] which results in a low blueshift with higher injection current density.^[21] As 368.5 nm UV-A wavelength is very close to the GaN emission wavelength of 365 nm, this may result in asymmetric emission spectra, which indicates that there may be absorption and re-emission of the UV light by the *p*-GaN layers. This finding on this micro-LED study aligned with previous reports on normal-sized UV-A LEDs.^[28] In this study, the size independence of emission wavelength and FWHM was further proved with experimental results.

In **Figure 4**, the on-wafer EQE versus current density has been shown for device size 8 × 8 to 100 × 100 μm². Devices demonstrated high on-wafer EQEs around 5.5%, with less than 0.5% difference among all the sizes at 100 A cm⁻². This result indicated that we successfully suppressed the leakage current of smaller sized micro-LEDs and achieved similar performance of smaller sized micro-LEDs to the regular-sized micro-LEDs.

It should be noted that the on-wafer EQE is expected to be significantly lower than the EQE obtained from a fully packaged LED measured in an integrating sphere.^[20,37] This result, to our knowledge, is the highest reported on-wafer EQE of UV-A micro-LEDs with a size smaller than 10 × 10 μm². Devices with the size of 15 × 15 μm² showed the highest EQE among all sizes (5.78% at 200 A cm⁻²). There is no direct relation found between the

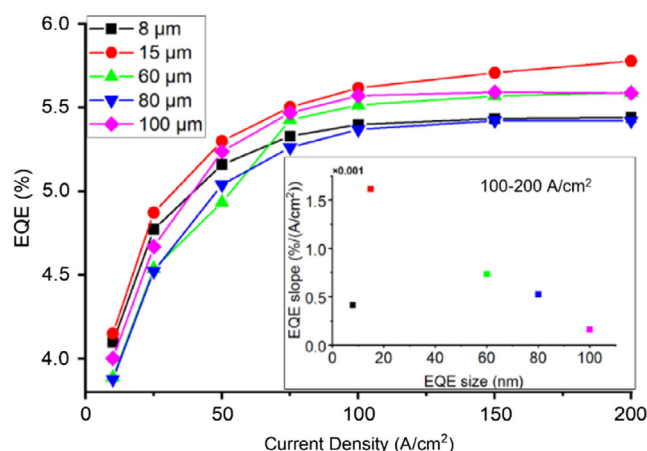


Figure 4. On-wafer EQE of device size 8 × 8, 15 × 15, 60 × 60, 80 × 80, and 100 × 100 μm².

EQE and the device size at current density <100 A cm⁻². However, as the injection current density is larger than 100 A cm⁻², majority of the devices (except 8 × 8 μm²) demonstrate that the EQE versus *J* slope (100–200 A cm⁻²) of the small-sized micro-LEDs seems to be larger than the regular-sized micro-LEDs. This indicates the efficiency droop is shifted to a higher current density (>200 A cm⁻²) for smaller sized micro-LEDs, which is possibly due to the combination of improved heat dissipation and slight larger sidewall damage, leading to an increased nonradiative recombination in the smaller device.^[38] Increased leakage currents result in higher nonradiative recombination, causing both a peak efficiency shift and a decrease in overall efficiency due to dominated Auger recombination.^[39] With the same leakage, higher efficiency was expected in smaller sized micro-LEDs due to better light extraction efficiency and heat dissipation.^[8–12] In this work, similar EQEs were observed

with different device sizes, which indicated the reduced efficiency in smaller devices was possibly compensated with the heat dissipation advantage.

Furthermore, there was no efficiency droop observed during 0–200 A cm^{−2}. This behavior might be attributed to successful Al₂O₃ passivation down to at least 15 μm micro-LED.^[29,30] For 8 × 8 μm² LED at higher current density (>100 A cm^{−2}), there may be an increase in nonradiative carrier recombination caused by defects at the sidewall leading to lower EQE versus *J* slope.

4. Summary and Conclusions

A systematic UV-A-ranged micro-LEDs study ranging from 8 × 8 to 100 × 100 μm² was presented and evaluated experimentally through optical and electrical performance. ALD passivation resulted in suppression of sidewall damage, leading to a low leakage current in both reverse and forward bias for all LEDs. Devices showed size-independent high on-wafer EQE of ≈5.5% for all devices at 100 A cm^{−2}. Smaller sized micro-LEDs showed a delayed efficiency droop in comparison with larger micro-LEDs, which indicated improved heat dissipation of small-sized micro-LEDs at higher current density. This article identifies the ALD passivation step as the key factor for the elimination of leakage current. Without the leakage current, smaller sized micro-LEDs experimentally showed the theoretical benefit of reduced current crowding and improved heat dissipation, indicating their potential to achieve high-power advanced optical devices.

Acknowledgements

The authors gratefully acknowledge use of facilities and instrumentation at the UW-Madison Wisconsin Centers for Nanoscale Technology (wcnt.wisc.edu) partially supported by the NSF through the University of Wisconsin MRSEC (DMR-1720415). This material is based upon work supported by the National Science Foundation under grant ECCS-2338683.

Conflict of Interest

The authors declare no conflict of interest.

Data Availability Statement

The data that support the findings of this study are available from the corresponding author upon reasonable request.

Keywords

EQE, Gallium nitride, Microfabrication, Micro-LEDs, UV LEDs

Received: April 8, 2024

Revised: May 17, 2024

Published online:

- [1] M. Kneissl, in *III-Nitride Ultraviolet Emitters: Technology and Applications* (Eds: M. Kneissl, J. Rass), Springer International Publishing, Cham **2016**, pp. 1–25.

- [2] Y. Muramoto, M. Kimura, S. Nouda, *Semicond. Sci. Technol.* **2014**, *29*, 084004.
- [3] D. Morita, M. Sano, M. Yamamoto, T. Murayama, S. Nagahama, T. Mukai, *Jpn. J. Appl. Phys.* **2002**, *41*, L1434.
- [4] M. Kneissl, T.-Y. Seong, J. Han, H. Amano, *Nat. Photonics* **2019**, *13*, 233.
- [5] T. Wu, C.-W. Sher, Y. Lin, C.-F. Lee, S. Liang, Y. Lu, S.-W. Huang Chen, W. Guo, H.-C. Kuo, Z. Chen, *Appl. Sci.* **2018**, *8*, 1557.
- [6] K.-L. Liang, W.-H. Kuo, H.-T. Shen, P.-W. Yu, Y.-H. Fang, C.-C. Lin, *Jpn. J. Appl. Phys.* **2020**, *60*, SA0802.
- [7] L. He, W. Zhao, K. Zhang, C. He, H. Wu, N. Liu, W. Song, Z. Chen, S. Li, *Opt. Lett.*, **OL** **2018**, *43*, 515.
- [8] Z. Gong, S. Jin, Y. Chen, J. McKendry, D. Massoubre, *J. Appl. Phys.* **2010**, *107*, 013103.
- [9] H. W. Choi, M. D. Dawson, P. R. Edwards, R. W. Martin, *Appl. Phys. Lett.* **2003**, *83*, 4483.
- [10] Z. Gong, H. X. Zhang, E. Gu, C. Griffin, M. D. Dawson, V. Poher, G. Kennedy, P. M. W. French, M. A. A. Neil, *IEEE Trans. Electron Dev.* **2007**, *54*, 2650.
- [11] N. Lobo Ploch, H. Rodriguez, C. Stollmacker, M. Hoppe, M. Lapeyrade, J. Stellmach, F. Mehnke, T. Wernicke, A. Knauer, V. Kueller, M. Weyers, S. Einfeldt, M. Kneissl, *IEEE Trans. Electron Dev.* **2013**, *60*, 782.
- [12] A. Chakraborty, L. Shen, U. K. Mishra, *IEEE Trans. Electron Dev.* **2007**, *54*, 1083.
- [13] R.-H. Horng, C.-X. Ye, P.-W. Chen, D. Iida, K. Ohkawa, Y.-R. Wu, D.-S. Wu, *Sci. Rep.* **2022**, *12*, 1324.
- [14] M.-C. Wu, I.-T. Chen, *Adv. Photon. Res.* **2021**, *2*, 2100064.
- [15] M. S. Wong, C. Lee, D. J. Myers, D. Hwang, J. A. Kearns, T. Li, J. S. Speck, S. Nakamura, S. P. DenBaars, *Appl. Phys. Express* **2019**, *12*, 097004.
- [16] D. Hwang, A. J. Mughal, M. S. Wong, A. I. Alhassan, S. Nakamura, S. P. DenBaars, *Appl. Phys. Express* **2017**, *11*, 012102.
- [17] K. R. Son, V. Murugadoss, K. H. Kim, T. G. Kim, *Appl. Surf. Sci.* **2022**, *584*, 152612.
- [18] P. Kirilenko, D. Iida, Z. Zhuang, K. Ohkawa, *Appl. Phys. Express* **2022**, *15*, 084003.
- [19] Y. Wu, B. Liu, F. Xu, Y. Sang, T. Tao, Z. Xie, K. Wang, X. Xiu, P. Chen, D. Chen, H. Lu, R. Zhang, Y. Zheng, *Photon. Res.* **2021**, *9*, 1683.
- [20] S. S. Pasayat, C. Gupta, M. S. Wong, R. Ley, M. J. Gordon, S. P. DenBaars, S. Nakamura, S. Keller, U. K. Mishra, *Appl. Phys. Express* **2020**, *14*, 011004.
- [21] S. S. Pasayat, R. Ley, C. Gupta, M. S. Wong, C. Lynsky, Y. Wang, M. J. Gordon, S. Nakamura, S. P. Denbaars, S. Keller, U. K. Mishra, *Appl. Phys. Lett.* **2020**, *117*, 061105.
- [22] H. Yu, M. H. Memon, D. Wang, Z. Ren, H. Zhang, C. Huang, M. Tian, H. Sun, S. Long, *Opt. Lett.*, **OL** **2021**, *46*, 3271.
- [23] Z. Qian, S. Zhu, X. Shan, P. Yin, Z. Yuan, P. Qiu, Z. Wang, X. Cui, P. Tian, *J. Phys. D: Appl. Phys.* **2022**, *55*, 195104.
- [24] M. Tian, H. Yu, M. H. Memon, Z. Xing, C. Huang, H. Jia, H. Zhang, D. Wang, S. Fang, H. Sun, *Opt. Lett.* **2021**, *46*, 4809.
- [25] M. Kumar, in *Light-Emitting Devices, Materials, and Applications*, SPIE, Bellingham, WA **2019**, pp. 15–21.
- [26] C.-C. Lin, K.-L. Liang, H.-Y. Chao, C.-I. Wu, S. fang Lin, B.-M. Huang, C.-W. Huang, C.-C. Wu, W.-H. Kuo, Y.-H. Fang, *ACS Appl. Opt. Mater.* **2023**.
- [27] R. K. Singh, L.-H. Chen, A. Singh, N. Jain, J. Singh, C.-H. Lu, *Front. Nanotechnol.* **2022**, *4*, <https://www.frontiersin.org/articles/10.3389/fnano.2022.863312/full>.
- [28] M. Asad, Q. Li, M. Sachdev, W. S. Wong, *Nanotechnology* **2019**, *30*, 504001.
- [29] C. Gupta, C. Lund, S. H. Chan, A. Agarwal, J. Liu, Y. Enatsu, S. Keller, U. K. Mishra, *IEEE Electron Dev. Lett.* **2017**, *38*, 353.

- [30] M. S. Wong, D. Hwang, A. I. Alhassan, C. Lee, R. Ley, S. Nakamura, S. P. DenBaars, *Opt. Express* **2018**, 26, 21324.
- [31] S. W. Lee, D. C. Oh, H. Goto, J. S. Ha, H. J. Lee, T. Hanada, M. W. Cho, T. Yao, S. K. Hong, H. Y. Lee, S. R. Cho, J. W. Choi, J. H. Choi, J. H. Jang, J. E. Shin, J. S. Lee, *Appl. Phys. Lett.* **2006**, 89, 132117.
- [32] Y. Yao, H. Li, P. Li, C. J. Zollner, M. Wang, M. Iza, J. S. Speck, S. P. DenBaars, S. Nakamura, *Appl. Phys. Express* **2022**, 15, 064003.
- [33] K. Fan, J. Tao, Y. Zhao, P. Li, W. Sun, L. Zhu, J. Lv, Y. Qin, Q. Wang, J. Liang, W. Wang, *Results Phys.* **2022**, 36, 105449.
- [34] Z. Deng, Y. Jiang, W. Wang, L. Cheng, W. Li, W. Lu, H. Jia, W. Liu, J. Zhou, H. Chen, *Sci. Rep.* **2014**, 4, 6734.
- [35] Y. Maidaniuk, R. Kumar, *Appl. Phys. Lett.* **2021**, 118, 062104.
- [36] Z.-H. Zhang, W. Liu, Z. Ju, S. Tiam Tan, Y. Ji, Z. Kyaw, X. Zhang, L. Wang, X. Wei Sun, H. Volkan Demir, *Appl. Phys. Lett.* **2014**, 104, 243501.
- [37] P. Li, H. Li, M. S. Wong, P. Chan, Y. Yang, H. Zhang, M. Iza, J. S. Speck, S. Nakamura, S. P. Denbaars, *Crystals* **2022**, 12, 541.
- [38] J. Zhu, T. Takahashi, D. Ohori, K. Endo, S. Samukawa, M. Shimizu, X.-L. Wang, *Phys. Status Solidi A* **2019**, 216, 1900380.
- [39] Y.-Y. Li, F.-Z. Lin, K.-L. Chi, S.-Y. Weng, G.-Y. Lee, H.-C. Kuo, C.-C. Lin, *IEEE Photonics J.* **2022**, 14, 1.